

# The role of diffusion-weighted echo planar MRI in central nervous system infections regarding etiopathogeneses

Yılmaz Kiroğlu, Nevzat Karabulut, Alpay Alkan

## ABSTRACT

Neuroimaging constitutes an important component in the diagnosis of the underlying infectious agents in central nervous system (CNS) infections. Despite the recent advances in neuroimaging evaluation, the diagnosis of unclear infectious CNS diseases remains a challenge. Conventional magnetic resonance imaging (MRI) is used in routine practice to identify abnormal areas involved in CNS infections. More recent MRI techniques, such as diffusion-weighted imaging (DWI), provide additional helpful information in the assessment of CNS infectious lesions compared with conventional MRI. This pictorial essay summarizes the clinical role of DWI in the demonstration of CNS infections including meningitis, encephalitis and pyogenic infections, and determination of the lesions compared with conventional MRI on the basis of physiopathologic phases of the infections.

**Key words:** • diffusion-weighted MRI • infection • central nervous system

**C**entral nervous system (CNS) infections are severe, life-threatening inflammatory diseases of the brain that can occur at any age and are caused by a variety of agents. Magnetic resonance imaging (MRI) has been widely accepted as a sensitive imaging technique for detecting early changes in intracranial infections (1–3). Diffusion-weighted imaging (DWI) is being increasingly used in various diseases involving the brain and spine, especially to diagnose very early cerebral ischemia; its role in other conditions, including infection, is being explored (4, 5).

Meningitis, a serious CNS infection, is a frequently fatal disease. It may also lead to severe neurological impairment. Conventional imaging, including fluid-attenuated inversion recovery (FLAIR) and enhanced MR sequences, has been the procedure of choice in the evaluation of all intracranial infections, including meningitis (6). Distention of the subarachnoid space on computed tomography (CT) or MRI is the earliest finding in meningitis. Several days after the onset of infection, the pia covering the brain and the arachnoid lining the dura mater develop vascular congestion; contrast injection may demonstrate enhancement of these meninges (7, 8).

Complications of meningitis are cerebritis, infarction, brain abscess, subdural effusion, empyema, sinus thrombosis, ventriculitis, hydrocephalus, and encephalitis (2). The appearance of meningitis on DWI may reflect pathologic changes that vary with severity and phase of infection. Extra-axial fluid collections generally occur during acute infections. Subdural and epidural empyemas show high signal on DWI and low signal on apparent diffusion coefficient (ADC) map (2, 7). Arachnoiditis occurs in the acute phase of severe meningitis and is followed by vasculitis, with a reduction in the diameter of vascular lumen. Consequently, the vessel walls may become necrotic and undergo thrombosis, which can result in disturbance of vascular supply (9). This likely explains the profound early vascular complications seen in meningitis, with restricted diffusion and hyperintense signal on DWI (Fig. 1). The vasculopathy of subacute and chronic phases of severe meningitis is proliferative, leading to partial or total destruction of the internal elastic lamina, with reduction in the lumen of larger vessels. In the subacute phase, reduced ADC values usually start to increase within a week and continue to increase during the early chronic phase, leading to vasogenic edema (9) (Fig. 2).

Inflammation is usually restricted to the subarachnoid area in the mild form of meningitis and is not accompanied by severe vasculitis. There is no obstructive change in leptomeningeal vessels and no apparent ischemia on conventional MRI or DW-MRI. Therefore conventional sequences and DWI are usually normal in these patients (7, 9).

Transient corpus callosum splenium (CCS) lesions have been reported, though rarely, in meningitis (10, 11). Transient CCS lesions with

From the Department of Radiology (Y.K. drkiroglu@yahoo.com, N.K.), Pamukkale University Faculty of Medicine, Denizli, Turkey; and the Department of Radiology (A.A.), İnnonü University Faculty of Medicine, Malatya, Turkey.

Received 23 March 2009; revision requested 20 July 2009; revision received 22 July 2009; accepted 27 July 2009.

Published online 4 February 2010  
DOI 10.4261/1305-3825.DIR.2564-09.1

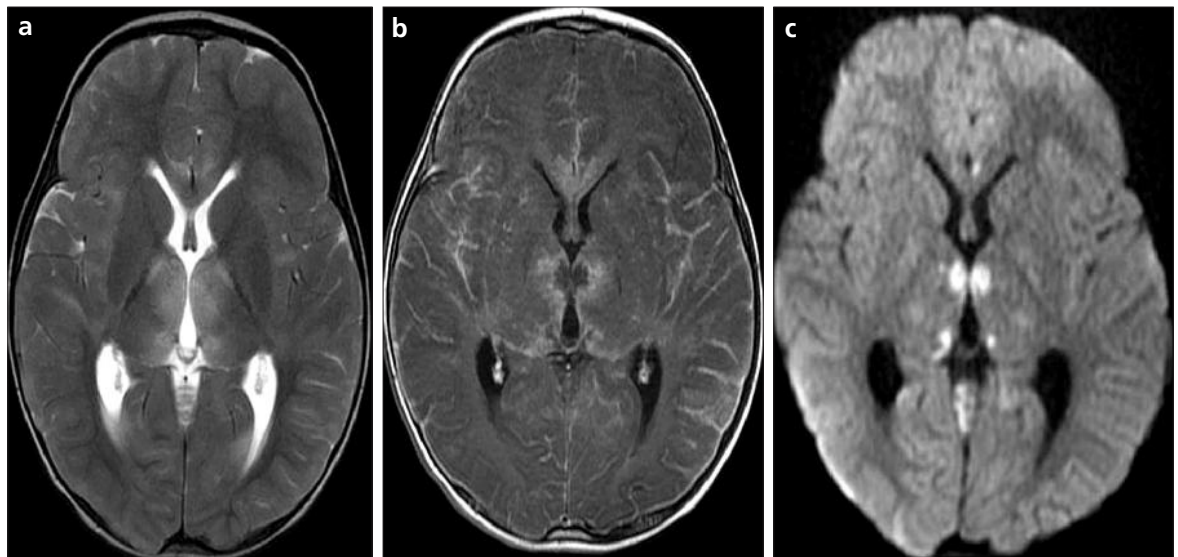


**Figure 1.** a–c. MRI of acute phase meningitis. T2-weighted fast spin-echo axial MR image (a) shows hyperintensities in the bilateral basal ganglia, thalamus, anterior callosal and superior vermian regions. Contrast-enhanced T1-weighted fast spin-echo axial MR image (b) shows intensive meningeal enhancement. DW ( $b = 1,000 \text{ s/mm}^2$ ) image (c) shows focal hyperintensities due to restricted diffusion in the corresponding sites, probably representing ischemic areas due to the early meningitic vascular complication.

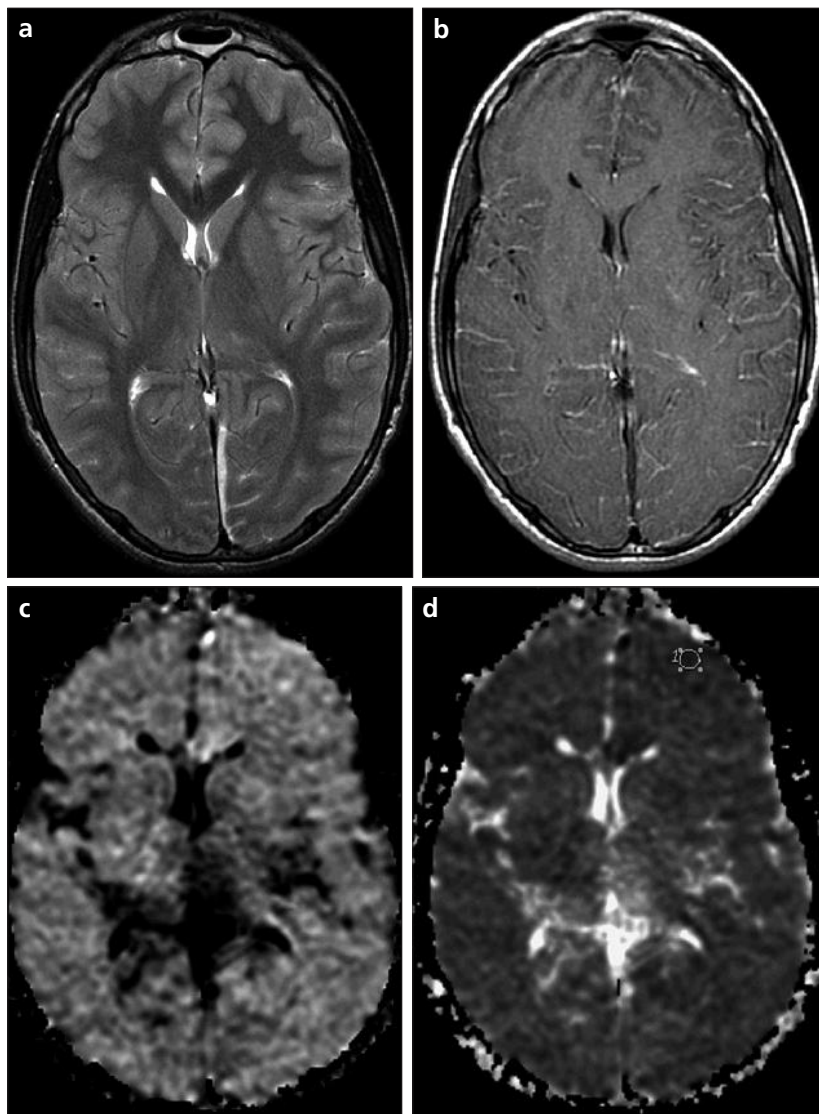


**Figure 2.** a–d. MRI of early subacute phase meningitis. T2-weighted fast spin-echo axial MR image (a) shows faint hyperintensities in bilateral thalamus. Contrast-enhanced T1-weighted fast spin-echo axial MR image (b) demonstrates widespread meningeal enhancement. DW ( $b = 1,000 \text{ s/mm}^2$ ) image (c) shows hyperintensities in the left frontal and anterior callosal areas and hypointensities in the bilateral basal ganglia and deep white matter. ADC map (d) shows hypointense and hyperintense areas corresponding to the restricted and unrestricted diffusion lesion sites. Note the subdural effusion in the posterior falx.

the mild form of *Haemophilus influenzae* meningitis usually lack contrast enhancement and represent reversal of restricted diffusion. Although the CCS derives its arterial supply from the carotid system, the absence of ischemic change in the same vascular territory eliminates a vascular etiology (12). This condition may be explained by limited direct invasion of neurons in CCS lesions or by insufficient immunologic response formation without a resultant rapid breakdown of the blood-brain barrier (10) (Fig. 3).

Encephalitis may be encountered as an isolated lesion or may be a part of meningoencephalitis. MR appearance of encephalitis on DWI is related to pathologic changes that occur following infectious involvement. In the acute phase, there are areas of congestion, perivascular infiltration, and thrombus formation pathologically (13). These changes likely cause cytotoxic edema, which leads to restricted

diffusion and low ADC in acute phase of the illness (1, 8). DWI shows the encephalitic lesions more clearly and broadly than conventional images in this phase (Fig. 4). In the late acute and early subacute phase, the components of vasculitis and perivascular infiltration diminish, and ADC starts rising (14). This phase is also accompanied by vasogenic and interstitial edema, which is responsible for the lesion becoming visible on T2-weighted MR images. The encephalitic lesion areas are relatively equal on conventional and DW-MR images (Fig. 5). In the late subacute and chronic phases, necrosis and demyelination start to develop, which may be responsible for hyperintensity on T2-weighted images with higher ADC values. Encephalitic lesions in this phase show hyperintense signal changes on ADC map; high ADC values may represent the substitution of cytotoxic edema by vasogenic edema (8, 14) (Fig. 6).

Cerebritis is the earliest manifestation of a pyogenic cerebral infection and is characterized by edema and perivascular exudates; it usually occurs 2–3 days following inoculation by the causative pathogen (15). In this phase, ill-defined infected tissue is hyperintense on FLAIR and T2-weighted MR images, whereas contrast enhancement is absent or minimal on T1-weighted images (16). In cerebritis, DWI of pyogenic infections reveals restricted diffusion and low ADC values, which

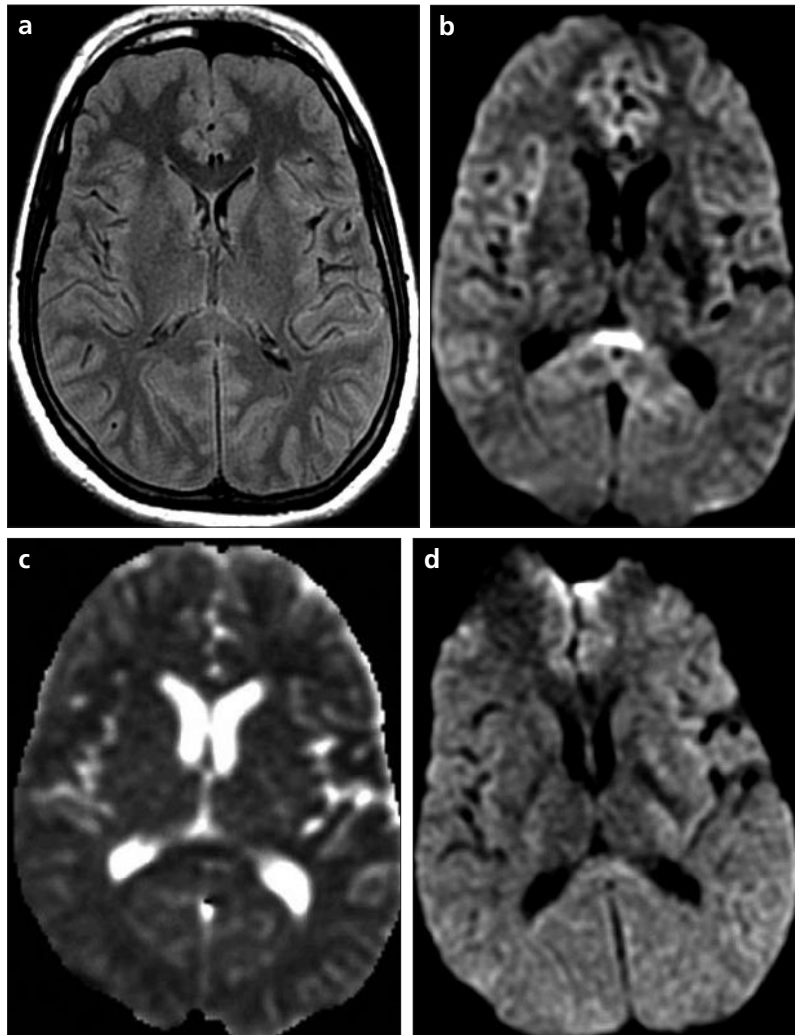


**Figure 3.** a–d. MRI of *Haemophilus influenza* meningitis. Axial FLAIR image (a) shows faint hyperintensities in the CCS. DW ( $b = 1,000 \text{ s/mm}^2$ ) image (b) shows focal hyperintensities in the CCS. ADC map (c) shows hypointensity corresponding to cytotoxic edema. DW ( $b = 1,000 \text{ s/mm}^2$ ) image after treatment (d) shows decreased hyperintensity in this area.

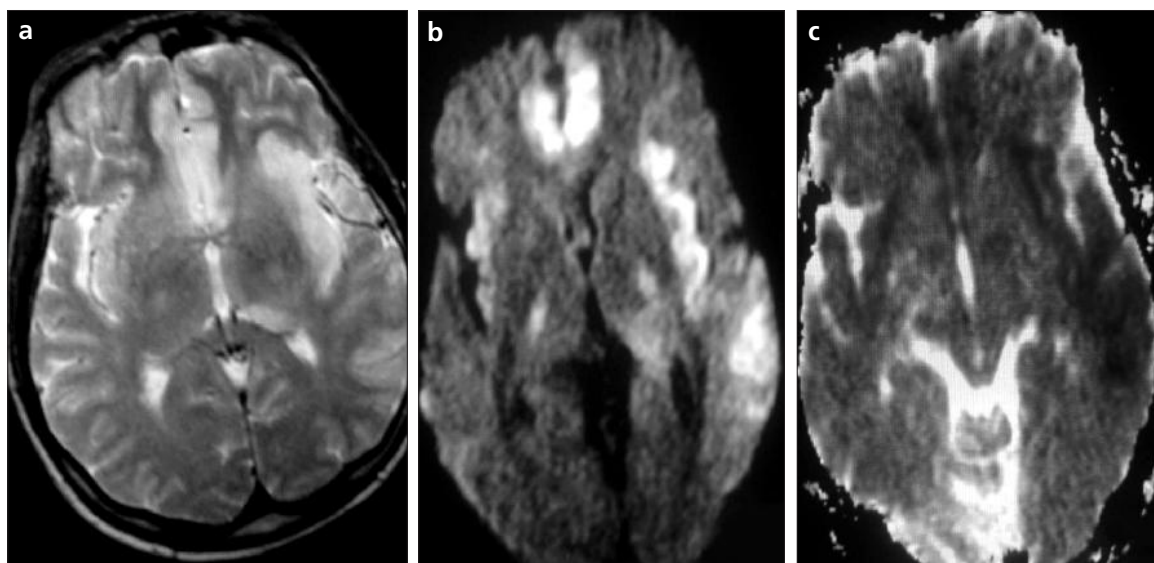


**Figure 4.** a–c. MRI of an acute phase viral encephalitis. T2-weighted fast spin-echo axial image (a) shows hyperintensities in the bilateral insular and left temporo-occipital cortex, cingulate gyri and left thalamus. DW ( $b = 1,000 \text{ s/mm}^2$ ) image (b) shows the borders of involved areas more clearly and extensively. ADC map (c) shows hypointensities in these areas due to restricted diffusion corresponding to cytotoxic edema.

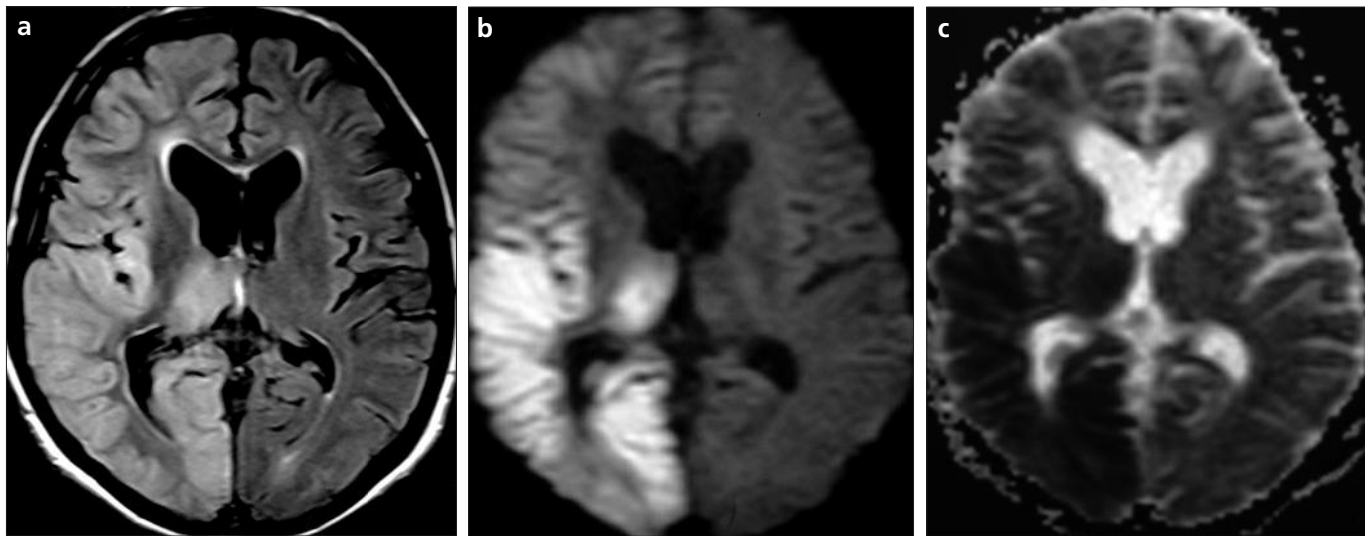


**Figure 5.** a–c. MRI of a subacute phase viral encephalitis. Axial FLAIR image (a) shows hyperintensities throughout the right cerebral hemisphere cortex and right thalamus. DW ( $b = 1,000 \text{ s/mm}^2$ ) image (b) shows hyperintensities and ADC map image (c) shows hypointensities due to restricted diffusion corresponding to cytotoxic edema in the same areas.

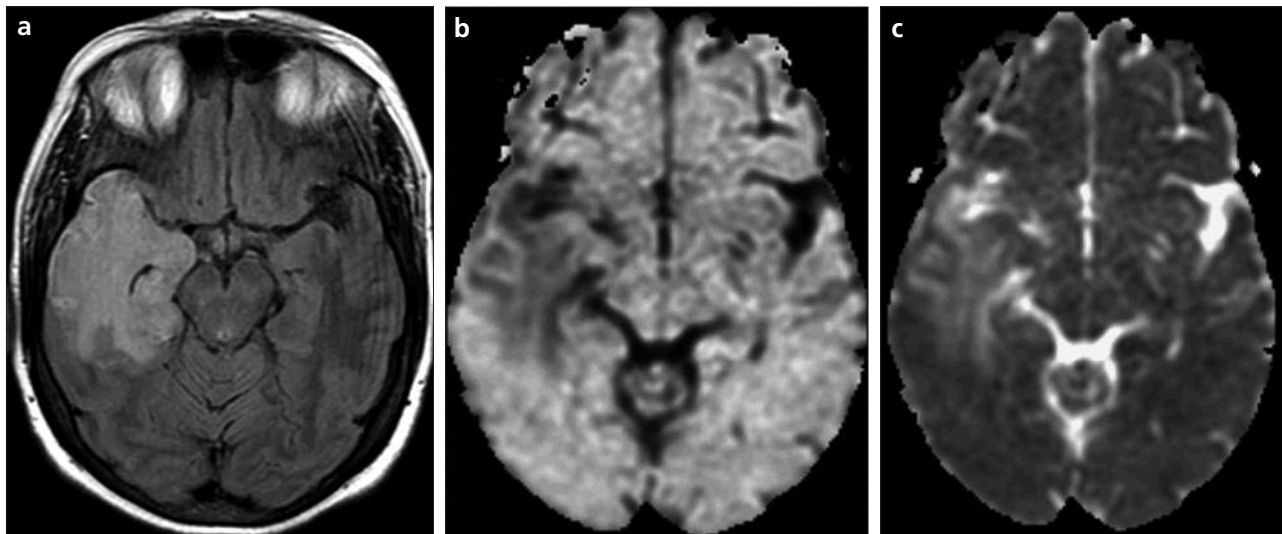


**Figure 6.** a–c. MRI of early chronic phase viral encephalitis. Axial FLAIR image (a) demonstrates hyperintensities in the right temporal lobe. DW ( $b = 1,000 \text{ s/mm}^2$ ) image (b) shows hypointensities and ADC map (c) shows hyperintensities due to increased diffusion corresponding to vasogenic edema in this area.

have been attributed to hypercellularity, brain ischemia, or cytotoxic edema without purulent fluid (17). However, it is unusual for patients to present at this phase of cerebral infection, and imaging of early cerebritis has not been widely reported.

Cerebritic lesions progress to capsule formation in the late phase of pyogenic infections. An ill-defined area of coagulative necrosis with a necrotic center transforms to characteristic capsular phase of abscess formation (18). There is a surrounding area of edematous parenchyma and blood vessels with perivascular exudates. The typical findings of capsular phase ab-

scess on conventional MR images are a mass lesion with a thin, smooth rim of contrast enhancement, and a variable degree of surrounding vasogenic edema (4). In this phase, pyogenic brain abscesses usually demonstrate hyperintense signal intensities on DW-MR images because of prolonged T2 relaxation time and markedly restricted water diffusion of suppurative fluid (19) (Fig. 7).

However, Krabbe et al. (20) reported that the signal intensity of pyogenic brain abscesses is not always high on DWI, and the ADC value may be higher than that of the normal brain parenchyma. Reddy et al. (21) report-

ed that restricted diffusion shown by ADC mapping is not pathognomonic for brain abscesses; in their report, 4% of abscesses showed higher ADC values than brain parenchyma. Gaviani et al. (3) reported that fungal cerebral abscesses are not pyogenic and that they may have histologic features of inflammation and necrosis rather than suppuration. Consequently, the features of DWI independent from the phase of the abscesses in certain cases and the different DWI findings in brain abscesses may be related to a difference in the viscosity of abscess fluid, which is determined by factors including variable concentrations of

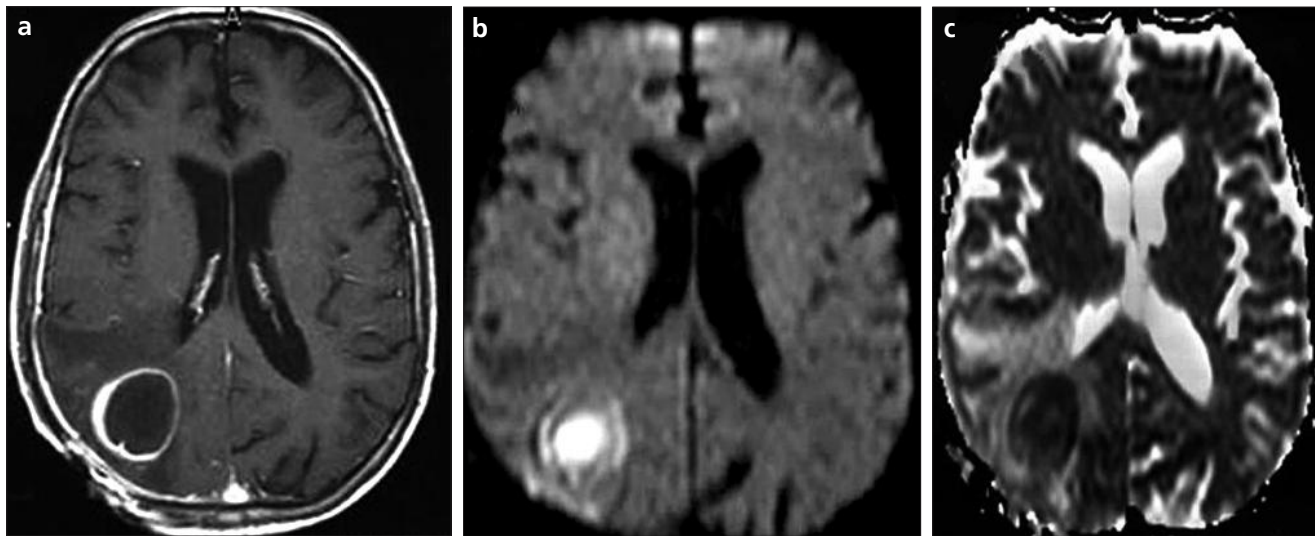


**Figure 7.** a–c. MRI of a brain abscess. Contrast-enhanced T1-weighted fast spin-echo axial image (a) shows a cystic lesion with peripheral enhancement in the right occipital region. DW ( $b = 1,000 \text{ s/mm}^2$ ) image (b) shows hyperintense central portion of the lesion and peripheral isointense areas. ADC map (c) shows hypointensity due to restricted diffusion in the central abscess zone with peripheral increased diffusion due to vasogenic edema.

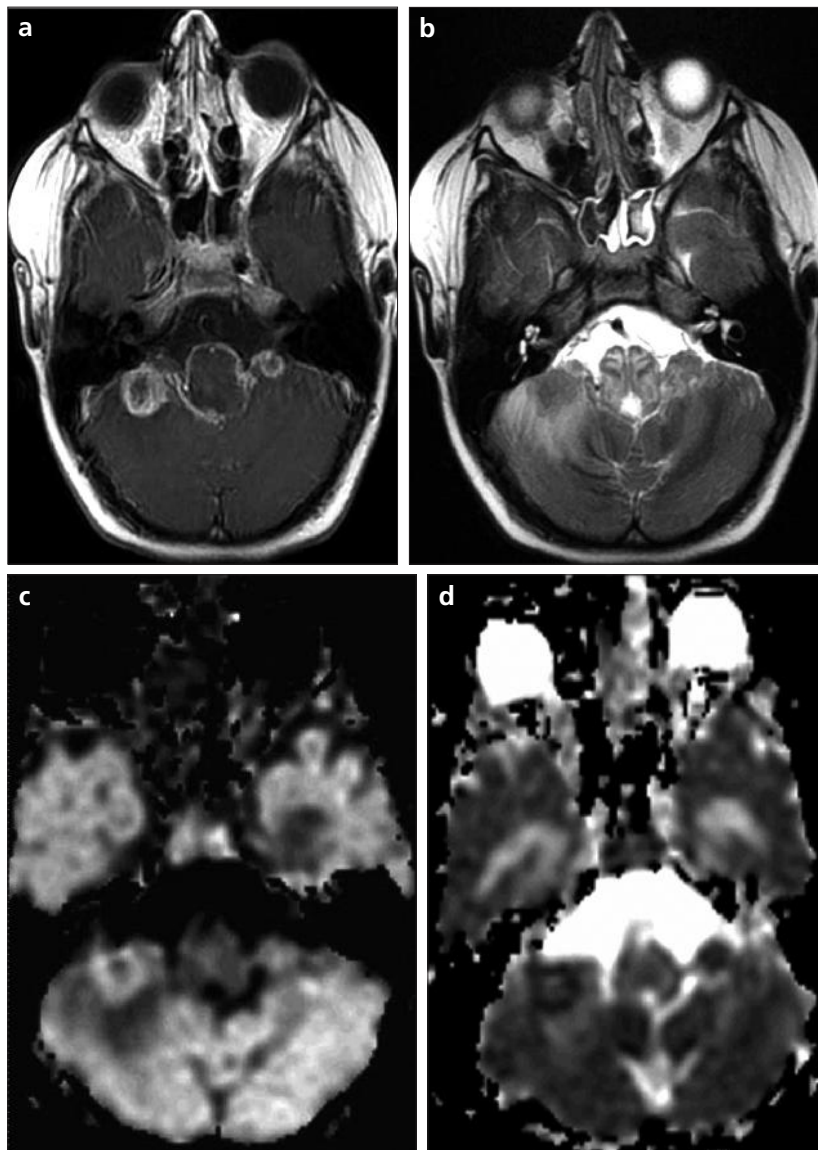


**Figure 8.** a–d. MRI of meningitis complicated with abscesses. Contrast-enhanced T1-weighted fast spin-echo axial image (a) shows irregular ring shaped enhancing abscesses with adjacent meninges in the bilateral anterior cerebellar regions. T2-weighted fast spin-echo axial image (b) shows isointense abscess areas with hyperintense peripheral edema. DW ( $b = 1,000 \text{ s/mm}^2$ ) image (c) shows hyperintensity in the left abscess and central hypointensity and peripheral hyperintensity in the right abscess. ADC map (d) shows unrestricted diffusion in the central part of the right abscess.

necrotic or viable inflammatory cells, causative organisms, and host immune response (5) (Fig. 8).

In conclusion, DWI is a simple form of examination to detect central nervous system infections and their complications. It is particularly effective in early identification of affected areas and may also contribute to the determination of disease phase.

#### References

1. Tsuchiya K, Katase S, Yoshino A, et al. Diffusion-weighted MR imaging of encephalitis. *AJR Am J Roentgenol* 1999; 173:1097–1099.
2. Kastrup O, Wanke I, Maschke M. Neuroimaging of infections. *NeuroRx* 2005; 2: 324–332.
3. Gaviani P, Schwartz RB, Hedley-Whyte ET, et al. Diffusion-weighted imaging of fungal cerebral infection. *AJR Am J Roentgenol* 2005; 26:1115–1121.
4. Mueller-Mang C, Castillo M, Mang TG, et al. Fungal versus bacterial brain abscesses: is diffusion-weighted MR imaging a useful tool in the differential diagnosis? *Neuroradiology* 2007; 49:651–657.

5. Lee EJ, Ahn KJ, Ha YS, et al. Unusual findings in cerebral abscess: report of two cases. *Br J Radiol* 2006; 79:156–161.
6. Mishra AM, Gupta RK, Saksena S, et al. Biological correlates of diffusivity in brain abscess. *Magn Reson Med* 2005; 54:878–885.
7. Smith RR. Neuroradiology of intracranial infection. *Pediatr Neurosurg* 1992; 2:92–104.
8. Kiroglu Y, Calli C, Yunten N, et al. Diffusion-weighted MR imaging of viral encephalitis. *Neuroradiology* 2006; 48:875–880.
9. Jan W, Zimmerman RA, Bilaniuk LT, et al. Diffusion-weighted imaging in acute bacterial meningitis in infancy. *Neuroradiology* 2003; 45:634–639.
10. Bulakbasi N, Kocaoglu M, Tayfun C, et al. Transient splenial lesion of the corpus callosum in clinically mild influenza-associated encephalitis/encephalopathy. *AJR Am J Roentgenol* 2006; 27:1983–1986.
11. Kobata R, Tsukahara H, Nakai A, et al. Transient MR signal changes in the splenium of the corpus callosum in rotavirus encephalopathy: value of diffusion-weighted imaging. *J Comput Assist Tomogr* 2002; 26:825–828.
12. Kakou M, Velut S, Destrieux C. Vascularisation arterielle et veineuse du corps calleux. *Neurochirurgie* 1998; 4(suppl):31–37.
13. Miyake M. The pathology of Japanese encephalitis. A review. *Bull World Health Organ* 1964; 30:153–160.
14. Prakash M, Kumar S, Gupta RK. Diffusion-weighted MR imaging in Japanese encephalitis. *J Comput Assist Tomogr* 2004; 28:756–761.
15. Flaris N, Hickey W. Development and characterization of an experimental model model of brain abscess in the rat. *Am J Pathol* 1992; 141:1299–1307.
16. Falcone S, Post MJ. Encephalitis, cerebritis and brain abscess: pathophysiology and imaging findings. *Neuroimaging Clin N Am* 2000; 10:333–353.
17. Tung GA, Rogg JM. Diffusion-weighted imaging of cerebritis. *AJR Am J Roentgenol* 2003; 24:1110–1113.
18. Jaggi RS, Husain M, Chawla S, et al. Diagnosis of bacterial cerebellitis: diffusion imaging and proton magnetic resonance spectroscopy. *Pediatric Neurology* 2005; 32:72–74.
19. Ebisu T, Tanaka C, Umeda M, et al. Discrimination of brain abscess from necrotic or cystic tumours by diffusion-weighted echo planar imaging. *Magn Reson Imaging* 1996; 14:1113–1116.
20. Krabbe K, Gideon P, Wagn P, et al. MR diffusion imaging of human intracranial tumours. *Neuroradiology* 1997; 39:483–489.
21. Reddy JS, Mishra AM, Behari S, et al. The role of diffusion-weighted imaging in the differential diagnosis of intracranial cystic mass lesions: a report of 147 lesions. *Surg Neurol* 2006; 66:246–250.